Phys. Lett. B 865 (2025) 139485

Contents lists available at ScienceDirect

Physics Letters B

journal homepage: www.elsevier.com/locate/physletb

Letter

Flavor dependence of charged pion fragmentation functions

H. Bhatt [a], P. Bosted [b], S. Jia [c], W. Armstrong [d], D. Dutta [a,*], R. Ent [e], D. Gaskell [e], E. Kinney [f], H. Mkrtchyan [g], S. Ali [h], R. Ambrose [i], D. Androić [j], C. Ayerbe Gayoso [a], A. Bandari [b], V. Berdnikov [h], D. Bhetuwal [a], D. Biswas [k], M. Boer [c], E. Brash [l], A. Camsonne [e], M. Cardona [c], J.P. Chen [e], J. Chen [b], M. Chen [m], E.M. Christy [k], S. Danagoulian [n], M. Diefenthaler [e], S. Covrig [e], B. Duran [c], M. Elaasar [o], C. Elliot [p], H. Fenker [e], E. Fuchey [q], J.O. Hansen [e], F. Hauenstein [r], T. Horn [h], G.M. Huber [i], M.K. Jones [e], M.L. Kabir [a], A. Karki [a], B. Karki [s], S.J.D. Kay [i,t], C. Keppel [e], V. Kumar [i], N. Lashley-Colthirst [k], W.B. Li [b], D. Mack [e], S. Malace [e], P. Markowitz [u], M. McCaughan [e], E. McClellan [e], D. Meekins [e], R. Michaels [e], A. Mkrtchyan [g], G. Niculescu [v], I. Niculescu [v], B. Pandey [k,w], S. Park [x], E. Pooser [e], B. Sawatzky [e], G.R. Smith [e], H. Szumila-Vance [e,u], A.S. Tadepalli [e], V. Tadevosyan [g], R. Trotta [h], H. Voskanyan [g], S.A. Wood [e], Z. Ye [d,y], C. Yero [u], X. Zheng [m]

[a] *Mississippi State University, Mississippi State, MS, 39762, USA*
[b] *The College of William & Mary, Williamsburg, VA, 23185, USA*
[c] *Temple University, Philadelphia, PA, 19122, USA*
[d] *Argonne National Laboratory, Lemont, IL, 60439, USA*
[e] *Thomas Jefferson National Accelerator Facility, Newport News, VA, 23606, USA*
[f] *University of Colorado Boulder, Boulder, CO, 80309, USA*
[g] *A.I. Alikhanyan National Science Laboratory, Yerevan Physics Institute, Yerevan, 0036, Armenia*
[h] *Catholic University of America, Washington, DC, 20064, USA*
[i] *University of Regina, Regina, Saskatchewan, S4S 0A2, Canada*
[j] *University of Zagreb, Zagreb, Croatia*
[k] *Hampton University, Hampton, VA, 23669, USA*
[l] *Christopher Newport University, Newport News, VA, 23606, USA*
[m] *University of Virginia, Charlottesville, VA, 22903, USA*
[n] *North Carolina A & T State University, Greensboro, NC, 27411, USA*
[o] *Southern University at New Orleans, New Orleans, LA, 70126, USA*
[p] *University of Tennessee, Knoxville, TN, 37996, USA*
[q] *University of Connecticut, Storrs, CT, 06269, USA*
[r] *Old Dominion University, Norfolk, VA, 23529, USA*
[s] *Ohio University, Athens, OH, 45701, USA*
[t] *University of York, Heslington, York, Y010 5DD, UK*
[u] *Florida International University, University Park, FL, 33199, USA*
[v] *James Madison University, Harrisonburg, VA, 22807, USA*
[w] *Virginia Military Institute, Lexington, VA, 24450, USA*
[x] *Stony Brook University, Stony Brook, NY, 11794, USA*
[y] *Tsinghua University, Beijing, 100084, China*

ARTICLE INFO

Editor: H. Gao

Keywords:
Charged pion multiplicities
Fragmentation functions
Charge symmetry violation

ABSTRACT

We have measured the flavor dependence of multiplicities for π^+ and π^- production in semi-inclusive deep-inelastic scattering (SIDIS) on proton and deuteron to explore a possible charge symmetry violation in fragmentation functions. The experiment used an electron beam with energies of 10.2 and 10.6 GeV at Jefferson Lab and the Hall-C spectrometers. The electron kinematics spanned the range $0.3 < x < 0.6$, $2 < Q^2 < 5.5$ GeV^2, and $2.2 < W < 3.2$ GeV. The pion fractional momentum range was $0.3 < z < 0.7$, and the transverse momentum range was $0 < p_T < 0.25$ GeV/c. Assuming factorization and allowing for isospin breaking, the results can be

* Corresponding author.
E-mail address: d.dutta@msstate.edu (D. Dutta).

https://doi.org/10.1016/j.physletb.2025.139485
Received 14 February 2025; Received in revised form 11 April 2025; Accepted 15 April 2025
Available online 17 April 2025

Higher twist corrections

described by two "favored" and two "unfavored" effective low p_T fragmentation functions that are flavor-dependent. We find each pair converges to a common flavor-independent fragmentation function at the highest W, where factorization is most applicable.

1. Introduction

Semi-inclusive deep-inelastic lepton-nucleon scattering ($lN \to l'hX$) is an excellent tool to study the quark hadronization mechanism described by fragmentation functions (FF) [1]. These FF describe how the quarks and gluons (partons) transform into color-neutral hadrons or photons during high-energy (hard) scattering processes. Pion semi-inclusive deep-inelastic scattering (SIDIS) is one such scattering process that allows access to the FF associated with the pions identified in the final state. These FF are the non-perturbative ingredient of the quantum chromodynamics (QCD) factorization theorems [2] used to analyze hard scattering processes and thereby provide insight into fundamental soft QCD quantities [3]. The FF are intimately connected to operator product expansion [4], with contributions from higher-order corrections that are suppressed by the power of the hard scale. With the improving accuracy of recent and upcoming experiments, these so-called "higher twist" corrections, such as the hadron mass correction, are becoming increasingly important [5]. The FF are also intrinsically linked to confinement in QCD, hence studies of FF are critical for a complete understanding of the basic properties of QCD, such as the dynamical generation of the mass, spin, and size of hadrons [6].

The current knowledge of pion FF are based on global QCD analyses [7–14] that are dominated by measurements from inclusive electron-positron (e^+e^-) annihilation into charged pions at very high energy scales (center-of-mass energy > 10 GeV). Inclusive e^+e^- annihilation is a clean process to study FF since it is independent of the parton distribution functions (PDF). However, it cannot distinguish between the light quark flavors or the quark and anti-quark FF. Thus, it cannot provide information about possible flavor dependence of FF – essential for a complete picture of FF and the spin structure of nucleons, in particular the transverse spin structure [15]. One of the most important advantages of SIDIS is the ability to constrain the flavor of the quark involved in the scattering process. Consequently, measuring the SIDIS process on the proton and deuteron allows an independent extraction of the flavor dependence of FF. The SIDIS experiments conducted over the last decade have convincingly established that the collinear picture of the quark-parton model is too simple, highlighting the importance of the transverse structure of the hadrons. The flavor structure of FF is important to understand the flavor dependence of the transverse-momentum-dependent (TMD) FF [15], and the relative differences between the observed single spin asymmetries of pions and kaons [16,17]. Thus, SIDIS measurements provide a unique capability to study the flavor structure of FF at an energy scale that is complementary to that of e^+e^- annihilation.

It is challenging to model FF as they are non-perturbative objects that cannot be deduced from first principles. Current models treat hadronization either as the sequential emission of hadrons from colored partons with emission probability parameterized to describe experimental data, such as the Lund string model [18], or approximate it as the emission of a single hadron and an on-shell spectator quark [19]. Another recent approach combines these two methods by calculating the emission probability within a QCD-inspired spectator model instead of a parameterization [20]. As charge conjugation symmetry (CC) and charge/isospin symmetry (CS/IS) are fundamental properties of QCD, most models of strong interaction processes use a simple quark flavor-independent (for light quarks) and isospin-independent ansatz. At the quark level, CS refers to the up (u) and down (d) quark interactions being identical when their mass difference is neglected [21]. It arises from the invariance of the QCD Hamiltonian under rotations about the 2-axis in isospin space, i.e. the interchange of u and d quarks while simultaneously interchanging protons and neutrons [22]. Therefore, CC and CS/IS allow one to drastically reduce the number of independent FF for the light quarks from eight to two [4].

The FF are expected to respect CS/IS to high precision since the fragmentation process is a dominantly strong interaction process. Most global fits of existing data that extract FF either assume CS or find no significant violation of CS [8,9]. On the other hand, the transverse polarization of the Λ hyperon in e^+e^- annihilation, as measured by the Belle Collaboration [23], seems to indicate a significant IS violation in the corresponding FF. Further, a recent analysis of the results from the HERMES experiment [24] has reported a non-zero flavor dependence of FF [25], posing a significant challenge to QCD. These results and the quest for TMD FF have created an urgent need for a systematic study of the flavor dependence of FF and their charge (isospin) symmetry violation (CSV). Such studies are critical, as they enable the planned high precision hadron tomography studies at current [26] and future facilities, such as the Electron-Ion Collider [27]. They are also essential for unraveling the dynamics of the parton-to-hadron transition, which may reveal novel aspects of the emergent hadron mass [28,29].

SIDIS is well suited for such studies, as the sum and difference ratio of π^+ and π^- production on proton to deuteron serves as an effective test of CS/IS. Further, the SIDIS reaction reflects higher twist contributions in the parton fragmentation sector, providing an effective tool to extract these contributions [30]. To exploit these advantages, a new SIDIS experimental program was undertaken at the upgraded JLab [31–33]. An integral part of this program, featuring measurements on both hydrogen (H) and deuterium (D) targets over a wide range of kinematics [31,32], was completed in 2019. In this letter, we report the results of the tests of charge and isospin symmetry violation and flavor dependence of the unpolarized FF extracted from the SIDIS experimental program. Any flavor dependence of FF could indicate the importance of higher twist corrections and help determine their size when included in global fits. These results can also be significant for other parts of the SIDIS program, such as the test of CSV in PDF [31].

The p_T-integrated (p_T is the pion transverse momentum relative to the virtual-photon direction) semi-inclusive pion electroproduction yield ($\frac{dN}{dz}$) as a function of the pion's longitudinal momentum fraction, z, is usually modeled as

$$\frac{dN}{dz} \sim \sum_i e_i^2 q_i(x,Q^2) D_{q_i\to\pi}(z,Q^2), \tag{1}$$

where the quarks of flavor i with charge e_i carrying a fraction x of nucleon momentum are represented by the PDF, $q_i(x,Q^2)$, and the spin averaged FF by $D_{q_i\to\pi}(z,Q^2)$. As a consequence of collinear factorization [2], the PDF are independent of z and FF are independent of x, but depend on the virtuality scale, or 4-momentum transferred squared (Q^2), via a logarithmic evolution [2,34].

We define the measured multiplicities for π^+ and π^- production from proton (p) and deuteron (d), $M^{\pi^\pm}_{\rm p/d}(x,Q^2,z)$, as the ratio of the respective SIDIS cross section to the inclusive DIS cross section (see Eq. S1 in the online Supplementary Material [35]). At leading order, assuming i) CS, ii) symmetric quark and anti-quark contributions from the sea, iii) identical p_T dependence of the measured multiplicities for charged pions from H/D targets, and iv) neglecting the strange quark contributions, the sum and difference ratios simplify to,

$$R_1(z) = \frac{M^{\pi^+}_{\rm d}(z) + M^{\pi^-}_{\rm d}(z)}{M^{\pi^+}_{\rm p}(z) + M^{\pi^-}_{\rm p}(z)} = 1 \tag{2}$$

and

$$R_2(z) = \frac{M_d^{\pi^+}(z) - M_d^{\pi^-}(z)}{M_p^{\pi^+}(z) - M_p^{\pi^-}(z)} = \frac{3\,(4u(x) + d(x))}{5\,(4u(x) - d(x))}, \tag{3}$$

where the $u(d)$ quark PDF are written as $u(x) = u_v(x) + \bar{u}(x)$ and $d(x) = d_v(x) + \bar{d}(x)$, with $u_v(d_v)$ and $\bar{u}(\bar{d})$ as the valence quark and sea anti-quark contributions, respectively. For measurements made in the valence region ($x > 0.3$) where the contributions from the sea quarks can be neglected, both ratios are independent of z and p_T. Thereby, these two ratios constitute an excellent test of CS within the collinear factorization formalism [2].

Most global analyses to extract PDF assume IS and CS in the PDF [11, 8], which reduces the number of independent PDF by half. If we assume CS in the PDF but allow for non-zero CSV in FF, the multiplicity $M_{p/d}^{\pi^\pm}(x, Q^2, z)$ for each target (H/D) and charged pion type can be written in terms of two favored FF, $D_{u\pi^+}(z)$, $D_{d\pi^-}(z)$, and two unfavored FF, $D_{d\pi^+}(z)$, $D_{u\pi^-}(z)$, respectively (see Eq. S2 in the online Supplementary Material [35]). Any difference between the two favored and the two unfavored FF is an indication of CSV in FF. The degree of CSV in the favored and unfavored FF can be quantified in terms of two parameters defined as:

$$\delta_{\rm CSV}^{f}(z) = \frac{D_{d\pi^-} - D_{u\pi^+}}{D_{u\pi^+}}, \quad \delta_{\rm CSV}^{uf}(z) = \frac{D_{d\pi^+} - D_{u\pi^-}}{D_{u\pi^-}} \tag{4}$$

Most current global analyses to extract FF either impose exact CS or arrive at CSV parameters that are effectively zero.

We have measured the four multiplicities integrated over $0 < p_T < 0.25$ GeV/c, for the electroproduction of $\pi^\pm$ from hydrogen and deuterium targets. These multiplicities, along with the PDF from a global fit of world data were used to extract the four FF. We have assumed an identical p_T dependence for the $\pi^\pm$ multiplicities from proton and deuteron, integrated over p_T with an average of $< p_T >= 0.1$ GeV/c. This assumption is confirmed by recent measurements [36]. The CSV of FF are then quantified in terms of the two parameters in Eq. (4).

2. The experiment

The experiment was carried out in the Fall of 2018 and the Spring of 2019, in Hall C at JLab. The experiment used the quasi-continuous wave electron beam with beam energies of 10.2 and 10.6 GeV and beam currents ranging from 2 μA to 70 μA. The scattered electrons were detected in the High Momentum Spectrometer (HMS) [37] in coincidence with the charged pions detected in the Super High Momentum Spectrometer (SHMS) [38]. In the electron spectrometer, a threshold gas Cherenkov detector and a segmented Pb-glass calorimeter [37] were used for electron identification. The pions in the hadron spectrometer were identified using the electron-hadron coincidence time, a heavy-gas threshold Cherenkov detector, an aerogel Cherenkov detector [39], and a segmented Pb-glass calorimeter [37]. Additional details of the experiment including the performance of the particle identification detectors are described in Sec. S-I of the Supplementary Material [35].

The experimental yields were obtained from the selected electron-pion coincidence events per milli-Coulomb of electrons incident on H, and D targets. The selected events passed cuts on momentum, scattering angles, and missing mass of the residual system, M_X, where M_X was restricted to be above the resonance region ($M_X > 1.6$ GeV/c^2). The yields were integrated over the azimuthalangle (ϕ) and p_T with an average of $< p_T > = 0.1$ GeV/c. The backgrounds from the target's aluminum windows and accidental coincidences were subtracted. This normalized SIDIS pion electroproduction yield was corrected for all known inefficiencies of the two spectrometers such as the detector efficiencies (97%–99%), trigger efficiency (98%-99%), tracking efficiencies, computer and electronic live times (94%–99%). The corrected yields were binned in z for 8 different kinematic settings (Table S1 of Supplementary Materials [35]) where the x ranged from 0.3 to 0.6, Q^2 ranged from 3.1 to 5.5 GeV^2 and the center-of-mass energy, W, ranged from 2.2 to 3.2 GeV. These ranges are complementary to previous experiments and constrained by the available maximum beam energy, the kinematic reach of the two spectrometers, and the desired statistical precision. A weighted average of settings with similar W and x reduced the 8 kinematic settings to 4.

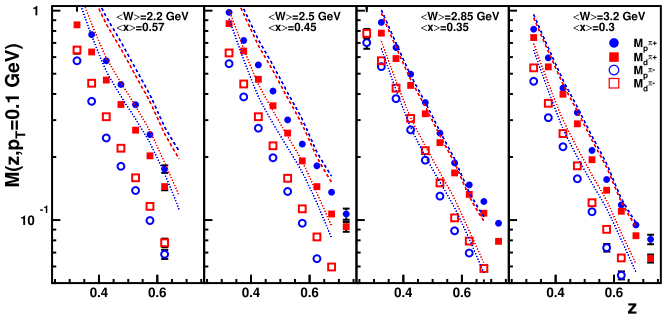

Fig. 1. The z dependence of the four p_T-integrated charged pion multiplicities; $M_p^{\pi^+}$ ($M_d^{\pi^+}$) solid circles (squares) and $M_p^{\pi^-}$ ($M_d^{\pi^-}$) open circles (squares). The panels are ordered from left to right in increasing values of W. All curves are from global fits by the MAP [13,44] collaboration integrated over the same p_T range as the experiment. The red (blue) dashed lines are for π^+ from H (D) target, while the dotted lines are for π^-.

3. Data analysis and results

A Monte Carlo (MC) simulation [40] of the SIDIS process was performed using a factorized model of the following form: $\sigma_{SIDIS} = \sigma_e \frac{d\sigma}{dz dp_T^2}$ where,

$$\frac{d\sigma}{dz dp_T^2} = \frac{b}{2\pi} e^{-bp_T^2} \frac{d\sigma}{dz}, \tag{5}$$

with $\frac{d\sigma}{dz}$ as in Eq. (1). The CTEQ5 next-to-leading-order (NLO) PDF were used to parametrize $q(x, Q^2)$ [41] along with a para-metrization of FF from fits to the z and p_T dependence of this and other Hall C 12 GeV data. It should be noted that a common value of b was used for π^+ and π^-, from both hydrogen and deuterium targets, since the p_T dependence, while not the primary focus of this analysis, was studied and observed to be the same for all cases.

While the MC is not GEANT-based, it does include radiative effects, multiple scattering, pion decay, and energy loss and has been demonstrated to accurately reproduce the performance of the Hall C spectrometers [42].

The MC was used to smear parameterized PDF and FF over the experimental acceptance. The MC included contributions due to radiative tails from exclusive pion electroproduction, pion and kaon decay, and electroproduction of ρ^0 mesons, and $\Delta(1232)$ resonances. Additional details about the models used in the simulation can be found in Refs. [42,43,36]. The MC yields were integrated over the same phase space as the measured yields. The diffractive ρ^0 contributions were subtracted from the experimental yields and ranged from 2% (at the lowest z) to about 10% (at the largest z) for the multiplicities. Their impact on the sum/difference ratios and the CSV parameters was negligible.

The corrected experimental yields (as described in Sec. 2), the Monte Carlo yield, and the model cross section at $p_T = 0.1$ GeV/c were used to obtain the four multiplicities, $M_{p/d}^{\pi^\pm}(z)$ shown in Fig. 1. These results confirm that the p_T dependence for the $\pi^\pm$ multiplicities from proton and deuteron are identical within the small p_T range covered, and the data agree better with global fits with increasing W. The sources of systematic uncertainty for the extracted multiplicities are listed in Table 1, and the total systematic uncertainty of 3.0 - 3.6% is the quadrature sum of these uncertainties.

The uncertainty in the target density for H (D) includes contributions from the uncertainty in the target length, thermal contraction, temperature, pressure, and the equation of state used to calculate the target density. The beam currents were adjusted to keep the event rates for π^+

Table 1
Systematic uncertainty of the multiplicities.

Source	Uncertainty (%)
Charge	0.45
Target related H (D)	0.8 (0.7)
Tracking & Live time	0.1
Particle identification	0.8
Background subtraction	0.2 - 2.0
Contamination	0.1
Acceptance	1.1
Kinematics	0.2
Radiative correction	1.1
Inclusive cross-section	2
FADC rate dependence	0.9
Total	3.0 - 3.6

and π^- similar, ensuring that the particle identification efficiency for π^+ and π^- were similar within the uncertainty. The systematic uncertainty in the event selection arising from the particle identification cuts was determined from the average variation in the experimental yield when the cuts were varied by a small fixed amount (typically ±10% of the nominal values) and variation between multiple equivalent analyses of the same data set.

The systematic uncertainty due to radiative correction was estimated from the average variation of the correction factor when the generation limits of the simulation of these radiative processes were varied and when the cross section models in the simulation were varied. The z correlated uncertainties in the models used to simulate Δ resonances, exclusive pion production, and ρ^0 meson production are the systematic uncertainty of the background subtraction procedure. They were estimated from the change in the simulated yield when the model parameters were varied. The systematic uncertainty due to the acceptance model in the Monte Carlo simulation was estimated from the variation of the multiplicity when the acceptance cuts were varied. The uncertainty in the inclusive cross section is from the latest fits to the world data [45]. Additional details about the experiment including how the systematic uncertainties were determined and their breakdown into different types are described in Sec. S-III of the Supplementary Material [35].

The four multiplicities were used to form the sum and difference ratios, which are shown as a function of z in Fig. 2 along with their statistical uncertainties. For the sum and difference ratios, many systematic uncertainties cancel to first order resulting in a net 2.2% systematic uncertainty shown by the magenta cross-hatched bands. The dotted lines are the expectations for models with CS/IS such as the fits by the JAM collaboration [11]. The dashed curves use FF from the global fits by the MAP [46] collaborations. The uncertainty for the JAM curves is not shown because, unlike the experiment and the MAP results, they are integrated over all p_T. At the highest W (3.2 GeV), the two ratios are remarkably independent of z over the entire range (z = 0.3 - 0.7) and are also consistent with the magnitude predicted by the global fits to existing data. In other words, the results agree with the CS/IS expectation. The sum ratio R_1 slowly but steadily deviates from the CS expectation with decreasing W (increasing x/Q^2), both in terms of the z independence and the magnitude. Similarly, the difference ratio also shows increasingly large deviations from the CS expectation with decreasing W. These deviations may indicate the importance of higher twist contributions to the SIDIS cross sections at low W and the potential of these measurements to help determine the higher twist contributions. These results also indicate that even for the limited range of p_T covered in this experiment, CS/IS seems to be valid for $W > 3$ GeV. Moreover, the sum/difference ratio from the previous JLab 6 GeV experiment [34] (shown as black triangles in the third and sixth panel) agrees remarkably well with the current results. These older ratios were obtained at the same $x = 0.32$, but at significantly lower W and Q^2 of 2.4 GeV and 2.3 GeV^2, respectively. This seems to indicate that x may also be relevant for tests of CS/IS.

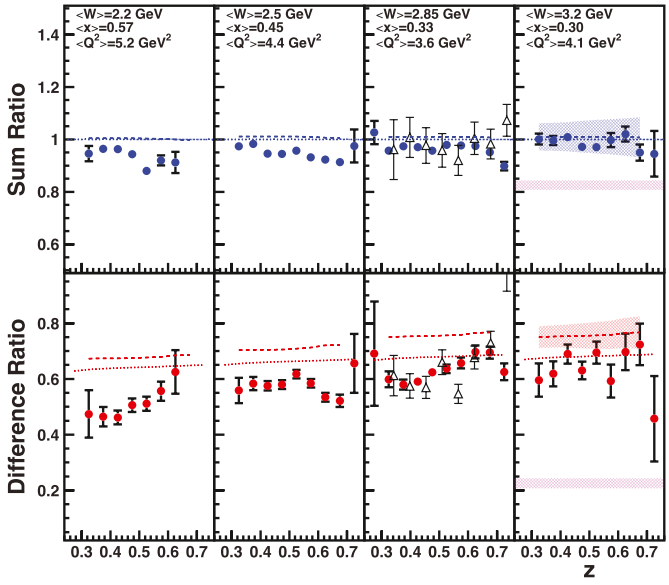

Fig. 2. The ratios $R_1(z)$ (top panels) and $R_2(z)$ (bottom panels) as a function of z. The panels are ordered left to right in increasing values of W. The dotted lines are the JAM [11] predictions which assume CS/IS. The dashed curves and the hatched bands are the ratios and their uncertainty from the MAP [46] collaboration. The magenta cross-hatched bands show the 2.2% systematic uncertainty of these ratios. The open triangles in the third panels show the ratios obtained from the previous JLab 6 GeV experiment [34].

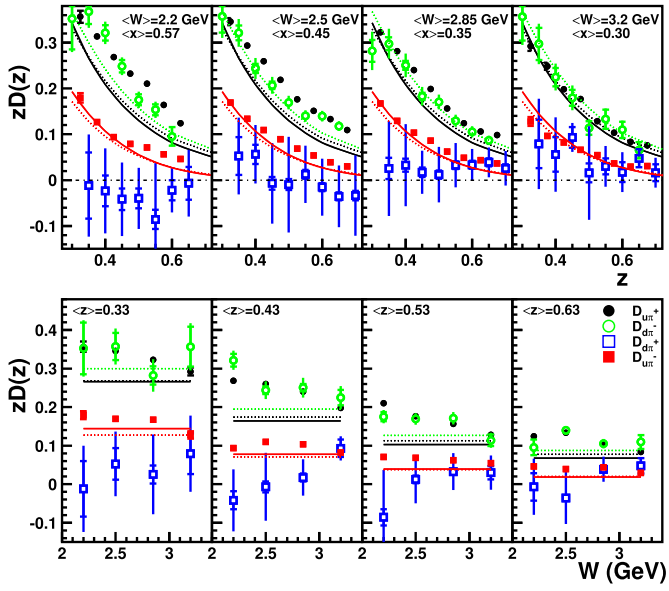

Fig. 3. The z dependence (top panels) and W dependence (bottom panels) of the two favored FF ($D_{u\pi^+}$ black solid and $D_{d\pi^-}$ green open, circles) and two unfavored FF ($D_{u\pi^-}$ red solid and $D_{d\pi^+}$ blue open, squares) extracted without assuming CS/IS. The panels are ordered left to right in increasing values of W. The inner error bars are the statistical uncertainty while the outer error bars are the total uncertainty. The solid (dashed) lines are FF from the JAM [11] (DSS [8,9]) collaborations. The open points have been shifted in z for clarity.

The four multiplicities were also used to obtain four FF ($D_{u\pi^+}(z)$, $D_{d\pi^-}(z)$ and $D_{u\pi^-}(z)$, $D_{d\pi^+}(z)$) by simultaneously solving a system of four equations as discussed earlier. The extracted FF are shown in Fig. 3 as a function of z (top panels) and W (bottom panels). Note that the JAM collaboration (solid lines) assumes CS/IS for all FF, while the DSS collaboration (dashed lines) assumes CS/IS only for the unfavored FF. The variation of the extracted FF due to the scale type uncertainties of

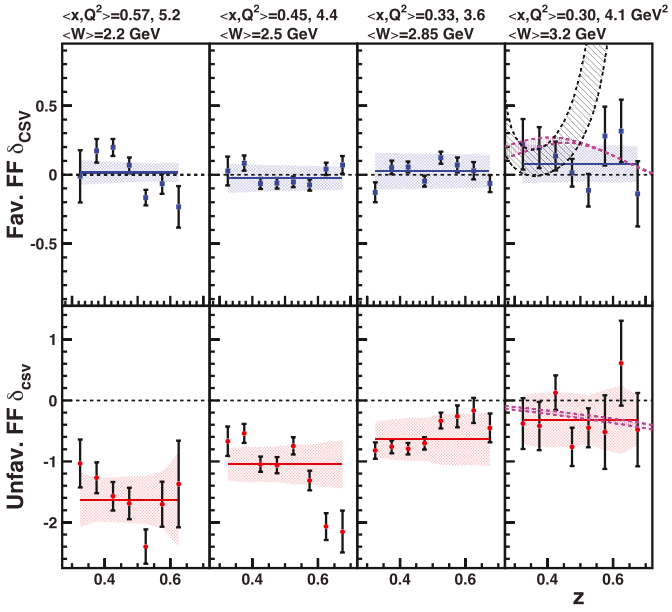

Fig. 4. The z dependence of the CS/IS violating parameter δ_{CSV} for the favored FF (top panels) and unfavored FF (bottom panels). From left to right, the panels are ordered in decreasing values of x (increasing W). The blue (red) solid lines are constant value fits to δ_{CSV}. The shaded bands are the systematic uncertainty. The black dashed lines are expectations assuming CS ($\delta_{CSV} = 0$). In the last panels, the magenta band with vertical hatching is the δ_{CSV} and its uncertainty from Peng and Ma [25], while the black band with angled hatching is from the MAP collaboration [46].

the multiplicities and the acceptance cuts was used to determine the systematic uncertainty of the FF. The statistical and systematic uncertainty of the unfavored FF, $D_{d\pi^+}(z)$, is significantly larger than all the other FF, because it is determined by the small differences in the flavor-dependent multiplicities, which amplify the uncertainties. However, within these large uncertainties, it is consistent with zero. The large fluctuations permit unphysical negative values seen at low W.

The two favored and two unfavored FF were used to form the favored and unfavored $\delta_{CSV}(z)$ parameters as defined in Eq. (4) and are shown in Fig. 4. The variation in the δ_{CSV} parameter due to the choice of PDF and scale type uncertainty was used to determine the systematic uncertainties of δ_{CSV}. The shaded bands show the systematic uncertainty. The favored δ_{CSV} parameter is essentially zero within the experimental uncertainties over the entire range of z and W. They are also consistent with the expectations of the global fits by Peng and Ma [25] but not with the unconstrained fits by the MAP collaboration [46].

4. Discussion

The statistical uncertainties of the unfavored δ_{CSV} parameter are significantly larger than those for the favored. Within these larger uncertainties, the unfavored δ_{CSV} is consistent with zero at the highest W but deviates from zero with decreasing W (increasing x). These results and the sum and difference ratios shown in Fig. 2 are a direct experimental confirmation of CS/IS for both the favored and unfavored FF at the highest W. The results confirm that for $W > 3$ GeV ($x \leq 0.35$), where factorization is most applicable, the FF are flavor-independent, and the fragmentation process obeys CS/IS within experimental uncertainties. The results also show a more complex fragmentation process at lower W (higher x), with possible contributions from higher-order corrections. As these corrections can arise from quark-quark or quark-gluon correlations, they can be flavor dependent. These results provide an opportunity to help estimate the higher-order corrections.

The poor statistics in the unfavored down quark fragmentation channel drive the larger uncertainty in the unfavored CSV parameter. Even in an isoscalar target, up quark scattering is a majority of the DIS cross section due to a larger electromagnetic coupling, and the poor statistics are exacerbated for SIDIS by the unfavored fragmentation configuration. Lacking a free neutron target, tagging the spectator (A-1) system would isolate hard scattering on the neutron. High-luminosity measurements with the spectator tagging of a proton or ^{3}He (using a D or ^{4}He target respectively) could significantly improve the uncertainties for unfavored down quark fragmentation.

5. Summary and outlook

In summary, we have measured the $\pi^{\pm}$ multiplicities from SIDIS on H and D targets over a wide range of kinematics. The sum and difference ratios of the four multiplicities satisfy CS/IS at the highest W (3.2 GeV) but steadily deviate from the CS expectation with decreasing W (increasing x). The multiplicities were used to quantify the flavor dependence of FF, they confirm the flavor independence of both the favored and unfavored FF at the highest W. The favored FF are flavor independent, within uncertainties, over the W range of the experiment. Within the larger experimental uncertainty, the flavor dependence of the unfavored FF increases with decreasing W. The results also indicate that higher-twist corrections are important for low W. When these data are included in future global fits of PDF and FF including higher-order corrections, they will provide further detailed insight into the fragmentation process. These results also suggest that CSV in FF is unlikely to interfere with the forthcoming extraction of CSV in PDF [31]. The spectator tagging technique pioneered at JLab can be used in future experiments to access nearly free neutron targets to improve the precision of the unfavored FF and their CSV.

Declaration of competing interest

None declared.

Acknowledgements

This work was funded in part by the U.S. Department of Energy, including contract AC05-06OR23177 under which Jefferson Science Associates, LLC operates Thomas Jefferson National Accelerator Facility, and by the U.S. Department of Energy Office of Science, contract numbers DE-AC02-06CH11357, DE-FG02-07ER41528, DE-FG02-96ER41003, and by the U.S. National Science Foundation grants PHY 2309976, 2012430 and 1714133 and the Natural Sciences and Engineering Research Council of Canada grant SAPIN-2021-00026. We wish to thank the staff of Jefferson Lab for their vital support throughout the experiment. We are also grateful to all granting agencies providing funding support to authors throughout this project.

Appendix A. Supplementary material

Supplementary material related to this article can be found online at https://doi.org/10.1016/j.physletb.2025.139485.

Data availability

Data will be made available on request.

References

[1] R.D. Field, R.P. Feynman, Phys. Rev. D 15 (1977) 2590.
[2] J.C. Collins, D.E. Soper, G. Sterman, Adv. Ser. Dir. High Energy Phys. 5 (1988) 1.
[3] S. Albino, Rev. Mod. Phys. 82 (2010) 2489.
[4] A. Metz, A. Vossen, Prog. Part. Nucl. Phys. 91 (2016) 136–202.
[5] A. Acardi, T. Hobbs, W. Melnitchouk, J. High Energy Phys. 11 (2009) 84.
[6] A. Acardi, A. Signori, Phys. Lett. B 798 (2019) 134993.
[7] M. Hirai, S. Kumano, T. Nagai, K. Sudoh, Phys. Rev. D 75 (2007) 094009.
[8] D. deFlorian, R. Sassot, M. Stratmann, Phys. Rev. D 75 (2007) 114010.

[9] D. deFlorian, R. Sassot, M. Epele, R.J. Hernández-Pinto, M. Stratmann, Phys. Rev. D 91 (2015) 014035.
[10] S. Albino, B. Kniehl, G. Kramer, Nucl. Phys. B 803 (2008) 42–104.
[11] E. Moffat, W. Melnitchouk, T.C. Rogers, N. Sato, Phys. Rev. D 104 (2021) 016015.
[12] A. Bacchetta, V. Bertone, C. Bissolotti, G. Bozzi, M. Cerutti, F. Piacenza, M. Radici, A. Signori, J. High Energy Phys. 10 (2022) 127.
[13] A. Bacchetta, V. Bertone, C. Bissolotti, G. Bozzi, M. Cerutti, F. Delcarro, M. Radici, L. Rossi, A. Signori, J. High Energy Phys. 08 (2024) 232.
[14] M. Cerutti, L. Rossi, S. Venturini, A. Bacchetta, V. Bertone, C. Bissolotti, M. Radici, Phys. Rev. D 107 (2023) 014014.
[15] A. Signori, A. Bacchetta, M. Radici, G. Schnell, J. High Energy Phys. 11 (2013) 194.
[16] A. Airapetian, et al., Phys. Rev. Lett. 103 (2009) 152002.
[17] C. Adolph, et al., Phys. Lett. B 744 (2015) 250.
[18] B. Andersson, G. Gustafson, G. Ingelman, T. Sjöstrand, Phys. Rep. 97 (1983) 31.
[19] P. Mulders, R. Tangerman, Nucl. Phys. B 461 (1996) 197.
[20] T. Ito, Phys. Rev. D 80 (2009) 074008.
[21] G. Miller, B. Nefkens, I. Šlaus, Charge symmetry, quarks and mesons, Phys. Rep. 194 (1990) 1.
[22] J.T. Londergan, S. Braendler, A.W. Thomas, Phys. Lett. B 424 (1998) 185.
[23] Y. Guan, et al., Phys. Rev. Lett. 122 (2019) 042001.
[24] A. Airapetian, et al., Phys. Rev. D 87 (2013) 074029.
[25] Q. Peng, B.-Q. Ma, Phys. Rev. C 107 (2023) 055202.
[26] J. Dudek, et al., Eur. Phys. J. A 48 (2012) 187.
[27] A. Acardi, et al., Eur. Phys. J. A 52 (2016) 268.
[28] H.Y. Xing, Z.Q. Yao, B.L. Li, D. Binos, Z.F. Cui, C.D. Roberts, Eur. Phys. J. C 84 (2024) 82.
[29] C.D. Roberts, D.G. Richards, T. Horn, L. Chang, Prog. Part. Nucl. Phys. 120 (2021) 103883.
[30] G. Xu, E. Hungerford, L. Pinsky, 2005.
[31] K. Hafidi, D. Gaskell, D. Dutta, et al., Jefferson Lab experiment E12-09-002.
[32] H. Mkrtchyan, P. Bosted, R. Ent, E. Kinney, et al., Jefferson Lab experiment E12-09-017.
[33] H. Avakian, et al., the CLAS12 collaboration, Run groups A and B.
[34] T. Navasardyan, et al., Phys. Rev. Lett. 98 (2007) 022001.
[35] See, Supplementary Material for a description of the experimental details including kinematic settings, data analysis methods, and systematic uncertainties.
[36] P. Bosted, et al., Transverse momentum and azimuthal dependence of charged pion multiplicities, publication in preparation.
[37] H. Mkrtchyan, et al., Nucl. Instrum. Methods A 719 (2013) 85.
[38] S. Ali, et al., The super high momentum spectrometer in hall-c, arXiv:2503.08706.
[39] T. Horn, et al., Nucl. Instrum. Methods A 842 (2017) 28.
[40] https://hallcweb.jlab.org/wiki/index.php/SIMC_Monte_Carlo.
[41] H.L. Lai, et al., Phys. Rev. D 55 (1997) 1280.
[42] H. Bhatt, PhD Dissertation, Mississippi State University, 2023, https://misportal.jlab.org/sti/publications/23431.
[43] S. Jia, PhD Dissertation, Temple University, 2022, https://misportal.jlab.org/sti/publications/21868.
[44] M. Cerutti, private communications, 2024.
[45] P.E. Bosted, M.E. Christy, Phys. Rev. C 77 (2008) 065206.
[46] LHAPDF, https://www.lhapdf.org.